

Published in final edited form as:

Macromolecules. 2010 ; 43(24): 10188–10190. doi:10.1021/ma1020209.

Stress Relaxation by Addition-Fragmentation Chain Transfer in Highly Crosslinked Thiol-Yne Networks

Hee Young Park¹, Christopher J. Kloxin¹, Timothy F. Scott¹, and Christopher N. Bowman^{1,2,*}

¹ Department of Chemical and Biological Engineering, Engineering Center, CB 424, University of Colorado, Boulder, CO 80309, USA

² Biomaterials Research Center, School of Dentistry, University of Colorado Health Sciences Center, Aurora, CO 80045, USA

Abstract

Radical mediated addition-fragmentation chain transfer of mid-chain allyl sulfide functional groups was utilized to reduce polymerization-induced shrinkage stress in thiol-yne step-growth photopolymerization reactions. In previous studies, the addition-fragmentation of allyl sulfide during the polymerization of a step-growth thiol-ene network demonstrated reduced polymerization stress; however, the glass transition temperature of the material was well below room temperature ($\sim -20^{\circ}\text{C}$). Many applications require super-ambient glass transition temperatures, such as microelectronics and dental materials. Polymerization reactions utilizing thiol-yne functional groups have many of the advantageous attributes of the thiol-ene-based materials, such as possessing a delayed gel-point, resistant to oxygen inhibition, and fast reaction kinetics, while also possessing a high glass transition temperature. Here we incorporate allyl sulfide functional groups into a highly crosslinked thiol-yne network to reduce polymerization-induced shrinkage stress. Simultaneous shrinkage stress and functional group conversion measurements were performed during polymerization using a cantilever-type tensometer coupled with a FTIR spectrometer. The resulting networks were highly crosslinked, possessed super-ambient glass transition temperatures, and exhibited significantly reduced polymerization-induced shrinkage stress when compared with analogous propyl sulfide-containing materials that are incapable of addition-fragmentation.

Polymerization of multifunctional monomers yields crosslinked polymeric networks (i.e., thermosets) that are extensively utilized in applications ranging from coatings and adhesives to dental materials and microelectronics^{1–3}. Unfortunately, these polymerizations are also typically accompanied by significant amounts of volumetric shrinkage⁴, where the associated stress that arises, leading to a wide range of deleterious effects such as material warping and cracking. Mitigation of this polymerization-induced shrinkage and/or the associated stress has been the focus of extensive research efforts over the past several decades^{5–6} and several methods, including ring-opening polymerization⁷, thiol-ene polymerizations⁸, and polymerization-induced phase separation⁹.

One approach to mitigate shrinkage stress was recently conceived whereby minimization of polymerization shrinkage itself is not directly addressed. Rather, the network connectivity continuously rearranges during the polymerization, thus promoting network relaxation and alleviating polymerization shrinkage stress to establish these materials as covalent adaptable networks^{10–11}. This network connectivity rearrangement approach is realized via radical-

*Corresponding author, christopher.bowman@colorado.edu.

mediated, addition—fragmentation chain transfer (i.e., AFCT) that occurs through the crosslinking strands. Thus, the network is rearranged without a concomitant change in network chemistry or crosslink density, while simultaneously being compatible with radical-mediated polymerizations. Although our approach was capable of dramatically reducing the polymerization shrinkage induced stress in elastomeric networks,¹⁰ demonstrating its effectiveness in glassy materials would vastly broaden its utility.

Our previous work exploiting AFCT-mechanisms to reduce polymerization stress utilized thiol-ene networks, whereby multifunctional thiol and vinyl monomers were copolymerized via a radical-mediated step-growth reaction mechanism to incorporate an allyl sulfide functionality^{12–13} in the crosslinking strands.¹⁰ Thiol-ene polymerizations possess many desirable attributes, such as extraordinary resistance to oxygen inhibition (owing to the facile abstractability of the thiol hydrogen)^{14–15} and rapid polymerization kinetics; moreover, its step-growth nature produces a homogeneous, crosslinked material with uniformly distributed allyl sulfide functional groups throughout the network. Unfortunately, thiol-ene polymerizations often yield elastomeric materials with low glass transition temperatures (T_g s) that are ill-suited for structural applications. Utilization of the thiol-yne polymerization mechanism (i.e., replacing the vinyl-based monomer with an ethynyl-based monomer) preserves the desirable characteristics of the thiol-ene mechanism while effectively doubling the crosslink density, yielding a concomitant increase in the T_g .^{16–19} Here, we incorporate allyl sulfide functional groups into thiol-yne networks to effect stress relaxation in super-ambient T_g materials.

The allyl sulfide AFCT functionality was incorporated in a thiol-yne system via the formulation of an allyl sulfide-based diethynyl monomer (2-methylene-propane-1,3-di(thiobut-1-yne) – MDTBY – Figure 1A) with a tetrathiol (pentaerythritol tetrakis(3-mercaptopropionate) – PETMP – Figure 1C) at a 1:2 ethynyl/thiol stoichiometric ratio, as each ethynyl group is capable of reacting with two thiol groups. For comparison, an analogous thiol-yne network was fabricated utilizing a propyl sulfide-based diethynyl monomer (2-methyl-propane-1,3-di(thiobut-1-yne) – MeDTBY – Figure 1B), where the propenyl sulfide is incapable of undergoing the AFCT-mediated relaxation mechanism, in place of MDTBY. These resins were additionally formulated with 3 wt% UV photoinitiator (1-hydroxycyclohexylphenylketone – HCPK – Figure 1D) to initiate the thiol-yne polymerization upon UV irradiation. Shrinkage stress and functional group conversion were monitored simultaneously using tensometry^{8, 20} and Fourier transform infrared (FTIR) spectroscopy during the photopolymerization of each resin (see Supporting Information).

The thiol-ene reaction follows an elegant mechanism of sequential propagation and chain transfer events, whereby addition of a thiyl radical to a vinyl functional group yields a carbon-centered radical that subsequently abstracts a thiol hydrogen, regenerating the thiyl radical and producing a thioether (Figure 2, cycle B). Utilization of an ethynyl-based monomer (i.e., thiol-yne) increases the polymerization reaction complexity as the mechanism proceeds via two sequential thiol addition reactions (Figure 2, cycles A and B). Incorporation of the allyl sulfide further increases the reaction complexity and provides a route for network connectivity rearrangement via the AFCT reaction, whereby a thiyl radical adds to an allyl sulfide functional group to yield an unstable carbon-centered radical intermediate, the fragmentation of which regenerates both the allyl sulfide functional group and the thiyl radical (Figure 2, cycle C). Whereas MeDTBY participates exclusively in the thiol-yne polymerization reaction (i.e., Figure 2, cycle A and B), MDTBY participates in both the thiol-yne polymerization and AFCT network connectivity rearrangement reactions concurrently (i.e., Figure 2, cycles A, B, and C). Thus, MeDTBY acts as a negative control monomer possessing similar chemical structure and molecular weight.

The stress that accumulates during a polymerization is typically attributed to the extent of post-gelation shrinkage and the modulus of the polymerized material. A comparison of the thermomechanical properties of the fully cured allyl and propyl sulfide-based materials demonstrates excellent similarity between the two network structures in regard to their crosslink density and glass transition behavior, as expected given the molecular structures (Figure 3). More specifically, the onset of the thermal transition from a glassy to elastomeric material occurs at approximately the same temperature and the rubbery moduli, which are proportional to the crosslink density, are similar. The temperature at the $\tan \delta$ maximum (assigned here as the T_g)^{22–23} demonstrates that both allyl and propyl sulfide-based materials exhibit super-ambient T_g s (allyl sulfide-based system: $41 \pm 1^\circ\text{C}$, propyl sulfide-based system: $39 \pm 1^\circ\text{C}$). Overall, the similarity of these networks indicates that the propyl sulfide addition to the MeDTBY enables this system to serve as an excellent control for which the only significant differences in material behavior should all be related to the simultaneous AFCT-polymerization mechanism rather than differences in the network structure.

The IR spectroscopy of PETMP-MeDTBY indicates rapid consumption of the ethynyl functional group; however, the ethynyl consumption does not proceed to complete conversion, presumably owing to severely reduced molecular mobility resulting from vitrification (Figure 4A)²⁴. Conversely, the ethynyl consumption during the PETMP-MDTBY photopolymerization (i.e., the allyl sulfide-containing system) proceeds at a slower rate, attributable to the sequestration of radicals participating in the AFCT mechanism.¹⁰ Moreover, consumption of the allyl sulfide is observed during the PETMP-MDTBY photopolymerization (Figure 4A), in contrast to the idealized reaction mechanism detailed in Figure 2 (i.e., cycle C). Previous work in thiol-ene systems demonstrated a minor side reaction whereby the AFCT carbon-centered radical intermediate abstracts a thiol hydrogen, thus consuming a small fraction of both allyl sulfide and thiol¹⁰. In the current thiol-yne system (i.e., PETMP-MDTBY), a large fraction of the allyl sulfide is consumed during the polymerization (Figure 4A), presumably reacting with an equivalent amount of thiol and thus producing an ethynyl/thiol stoichiometric imbalance. This ethynyl/thiol imbalance results in a limited amount of ethynyl homopolymerization, effecting a mixed-mode step- and chain-growth polymerization mechanism¹⁸ that would be expected, in the absence of any other differences, to increase both the crosslinking density and the corresponding stress. Furthermore, homopolymerization results in a lower gel-point conversion, which would reduce the stress dissipated by pre-gelation viscous flow, further heightening the stress level expected in such a system. Thus, in the absence of any network relaxation associated with the AFCT-mediated relaxation mechanism, the photopolymerization of PETMP-MDTBY is expected to exhibit a much higher polymerization stress level as compared to PETMP-MeDTBY. In contrast, Figure 4B demonstrates the dramatic effect of the AFCT-mediated relaxation mechanism as the PETMP-MDTBY resin exhibits significantly reduced polymerization stress (43%) as compared to the PETMP-MeDTBY control, attributable to the allyl sulfide AFCT mechanism facilitating network connectivity rearrangement during the polymerization. This relaxation behavior is observed despite the glassy nature of the polymer networks that are formed.

In this study, we found that the incorporation of allyl sulfide functional groups in the polymer backbone of a material possessing a super-ambient T_g reduces polymerization-induced shrinkage stress, owing to network connectivity rearrangement via a AFCT mechanism. To our knowledge, this observation is the first successful demonstration of AFCT-mediated relaxation during the polymerization of a glassy polymer network to induce stress relaxation. As this approach is well-suited for incorporation in free radical polymerizations, or indeed any other thermosetting polymerization where radicals can be

generated, the mitigation of polymerization stress can be achieved even in high performance materials.

Supplementary Material

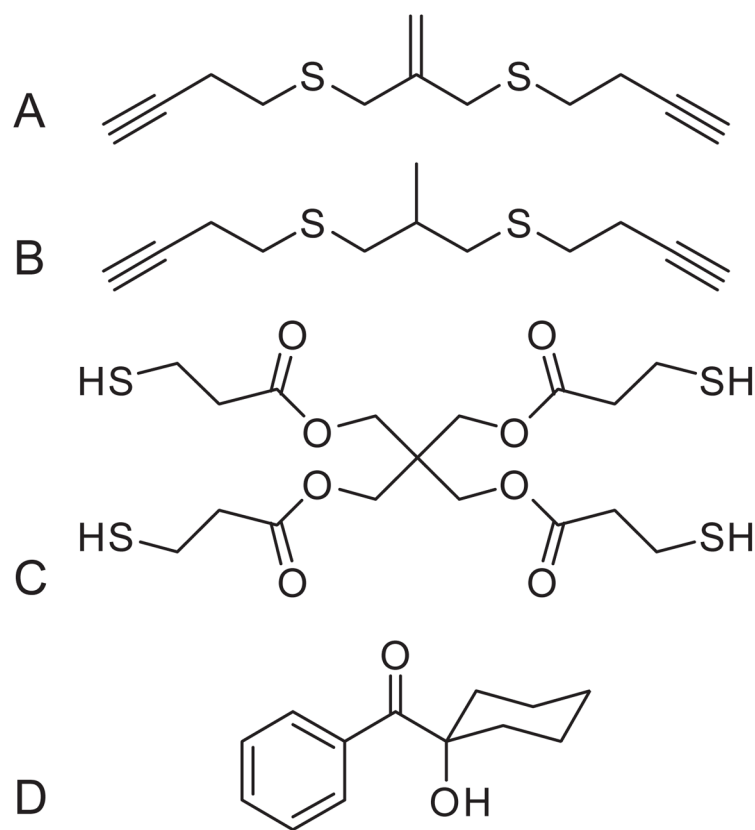
Refer to Web version on PubMed Central for supplementary material.

Acknowledgments

This investigation was supported by NIDCR 2 R01 DE-010959-11 from the National Institutes of Health and NSF 0933828.

References

1. Drury CJ, Mutsaers CMJ, Hart CM, Matters M, de Leeuw DM. *Appl Phys Lett*. 1998; 73:108–110.
2. Stansbury JW, Bowman CN, Newman SM. *Phys Today*. 2008; 61:82–83.
3. Yoffe AD. *Adv Phys*. 2001; 50:1–208.
4. Sanda F, Takata T, Endo T. *Macromolecules*. 1994; 27:1099–1111.
5. Davidson CL, Feilzer AJ. *J Dent*. 1997; 25:435–440. [PubMed: 9604575]
6. Francis LF, McCormick AV, Vaessen DM, Payne JA. *J Mater Sci*. 2002; 37:4717–4731.
7. Alcoutlabi M, McKenna GB, Simon SL. *J Appl Polym Sci*. 2003; 88:227–244.
8. Lu H, Carioscia JA, Stansbury JW, Bowman CN. *Dent Mater*. 2005; 21:1129–1136. [PubMed: 16046231]
9. Lu H, Trujillo-Lemon M, Ge J, Stansbury JW. *Compend Contin Educ Dent*. 2010; 31(Spec2):1–4. [PubMed: 20521567]
10. Kloxin CJ, Scott TF, Bowman CN. *Macromolecules*. 2009; 42:2551–2556. [PubMed: 20160931]
11. Kloxin CJ, Scott TF, Adzima BJ, Bowman CN. *Macromolecules*. 2010; 43:2643–2653. [PubMed: 20305795]
12. Moad G, Rizzardo E, Thang SH. *Australian Journal of Chemistry*. 2005; 58:379–410.
13. Meijjs GF, Rizzardo E, Thang SH. *Macromolecules*. 1988; 21:3122–3124.
14. Szmant HH, Mata AJ, Namis AJ, Panthanickal AM. *Tetrahedron*. 1976; 32:2665–2680.
15. Jacobine, AF. *Radiation Curing in Polymer Science and Technology*. Vol. 3. Elsevier Applied Science; London: 1993. p. 219–268.
16. Chan JW, Shin J, Hoyle CE, Bowman CN, Lowe AB. *Macromolecules*. 2010; 43:4937–4942.
17. Chan JW, Zhou H, Hoyle CE, Lowe AB. *Chem Mater*. 2009; 21:1579–1585.
18. Fairbanks BD, Scott TF, Kloxin CJ, Anseth KS, Bowman CN. *Macromolecules*. 2009; 42:211–217. [PubMed: 19461871]
19. Lowe AB, Hoyle CE, Bowman CN. *J Mater Chem*. 2010; 20:4745–4750.
20. Lu H, Stansbury JW, Dickens SH, Eichmiller FC, Bowman CN. *J Mater Sci-Mater M*. 2004; 15:1097–1103. [PubMed: 15516870]
21. Scott TF, Schneider AD, Cook WD, Bowman CN. *Science*. 2005; 308:1615–1617. [PubMed: 15947185]
22. Ferrillo RG, Achorn PJ. *J Appl Polym Sci*. 1997; 64:191–195.
23. Li G, Lee-Sullivan P, Thring RW. *J Therm Anal Calorim*. 2000; 60:377–390.
24. Cook WD. *Polymer*. 1992; 33:2152–2161.

**Figure 1.**

Materials used: (A) MDTBY, (B) MeDTBY, (C) PETMP, and (D) HCPK.

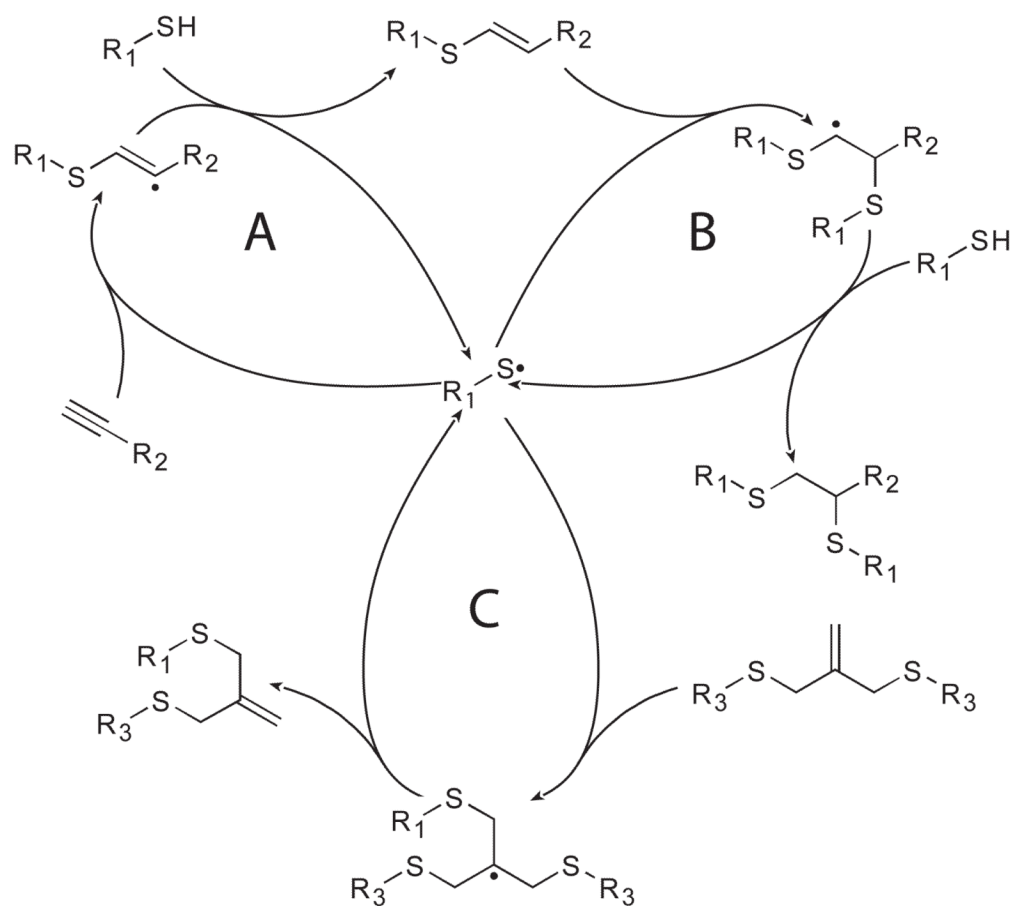


Figure 2. Schematic of concurrent thiol-yne (cycles A and B) and allyl sulfide AFCT (cycle C) mechanisms

The thiol-yne mechanism is comprised of two sequential addition events, whereby addition of a thiyl radical to an ethynyl functional group yields a vinyl sulfide functional group (cycle A); subsequent thiyl radical addition across this vinyl completes the thiol-yne polymerization mechanism (cycle B)¹⁸. Thiyl radical addition to and subsequent fragmentation of the allyl sulfide functional group conserves the concentrations of both the thiyl radical and allyl sulfide functional group (cycle C).^{10, 21}

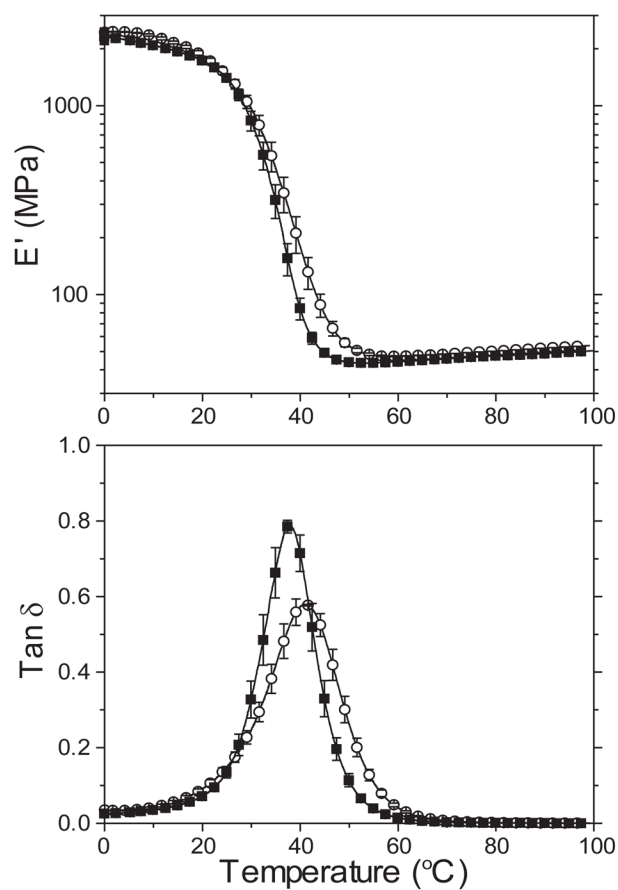


Figure 3. (A) Elastic modulus and (B) $\tan \delta$ versus temperature for stoichiometrically balanced mixtures of PETMP-MDTBY (○) and PETMP-MeDTBY (■)
Samples were formulated with 3 wt % HCPK and irradiated at 365 nm, 10 mW/cm², for 30 min.

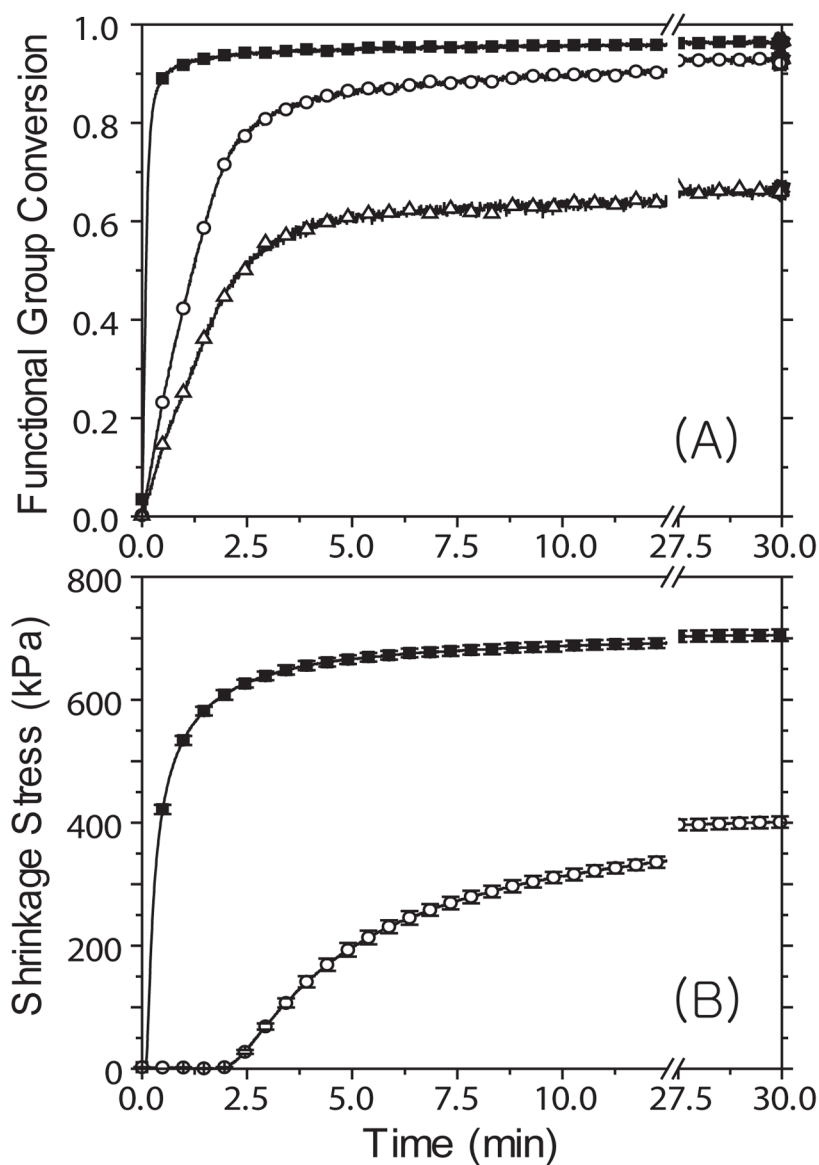


Figure 4. (A) Functional group conversion (ethynyl conversion of PETMP-MDTBY (○), ethynyl conversion of PETMP-MeDTBY (■), and allyl sulfide of PETMP-MDTBY (△)) and (B) polymerization shrinkage stress evolution (PETMP-MDTBY (○) and PETMP-MeDTBY (■)) versus time for a 2:1 stoichiometric mixture of thiol:yne
 Samples contain 3 wt% HCPK and were irradiated at 10 mW/cm² using 365 nm light.